

# Identification of Integrin $\beta$ Subunit Mutations that Alter Heterodimer Function In Situ<sup>D</sup>

Alison L. Jannuzi, Thomas A. Bunch, Robert F. West, and Danny L. Brower\*

Department of Molecular and Cellular Biology, and Department of Biochemistry and Molecular Biophysics, Arizona Cancer Center, University of Arizona, Tucson, Arizona 85724

Submitted February 2, 2004; Revised May 17, 2004; Accepted June 2, 2004  
Monitoring Editor: Jean Schwarzbauer

We conducted a genetic screen for mutations in *mysospheroid*, the gene encoding the *Drosophila*  $\beta$ PS integrin subunit, and identified point mutants in all of the structural domains of the protein. Surprisingly, we find that mutations in very strongly conserved residues will often allow sufficient integrin function to support the development of adult animals, including mutations in the ADMIDAS site and in a cytoplasmic NPXY motif. Many mutations in the I-like domain reduce integrin expression specifically when  $\beta$ PS is combined with activating  $\alpha$ PS2 cytoplasmic mutations, indicating that integrins in the extended conformation are unstable relative to the inactive, bent heterodimers. Interestingly, the screen has identified alleles that show gain-of-function characteristics in cell culture, but have negative effects on animal development or viability. This is illustrated by the allele *mys*<sup>b58</sup>; available structural models suggest that the molecular lesion of *mys*<sup>b58</sup>, V409>D, should promote the “open” conformation of the  $\beta$  subunit I-like domain. This expectation is supported by the finding that  $\alpha$ PS2 $\beta$ PS (V409>D) promotes adhesion and spreading of S2 cells more effectively than does wild-type  $\alpha$ PS2 $\beta$ PS, even when  $\beta$ PS is paired with  $\alpha$ PS2 containing activating cytoplasmic mutations. Finally, comparisons with the sequence of human  $\beta$ 8 suggest that evolution has targeted the “*mys*<sup>b58</sup>” residue as a means of affecting integrin activity.

## INTRODUCTION

The integrin cell surface receptors are critical for many morphogenetic events during animal development as well as numerous physiological events in adults, including many disease-related processes (Hynes, 2002). A major goal of integrin biology is understanding the molecular structure and dynamics of the integrin  $\alpha\beta$  heterodimer. Using conformation specific antibodies, it has been clear for many years that integrins undergo significant structural changes in response to binding of ligands or signals from within the cell. These and other studies led to various molecular models for integrin structure, but only recently have high-resolution x-ray, NMR, and electron microscope studies begun to elucidate in molecular detail how the  $\alpha$  and  $\beta$  subunits are organized.

A major advance in our understanding of integrin structure-function relationships was the determination of an x-ray structure for most of the extracellular part of  $\alpha v\beta 3$ . This revealed a compact integrin heterodimer, bent over with the ligand-binding head domains facing back toward the plasma membrane (Xiong *et al.*, 2001). Elegant electron microscopy studies have demonstrated that these x-ray images represent what has historically been called the inactive conformation and that activation stimulates the heterodimer to assume the extended posture where the head region is more accessible to fibrous extracellular matrix ligands (Takagi *et al.*, 2002). Further electron mi-

croscopy experiments have shown that there are additional steps in the full activation of the heterodimer, which lead to a movement of the most distal segment of the  $\beta$  subunit stalk (the hybrid domain) relative to the ligand binding I-like domain (Figure 1). This pivoting of the hybrid domain is thought to be driven by a tertiary structure change in the I-like domain (Liddington *et al.*, 2002; Luo *et al.*, 2003a, 2004; Mould *et al.*, 2003a, 2003b).

Many site-directed mutagenesis studies were performed on integrin extracellular and intracellular domains before there was much of an understanding of the heterodimer structure. Residues have been identified that are required for dimer formation, ligand binding, or association with intracellular proteins, but for the most part these studies have not pointed to specific molecular interactions in the extracellular region that can explain the movements of the integrin heterodimers. The detailed structures now available are beginning to lead to more incisive site-directed mutagenesis studies in this regard (e.g., Chen *et al.*, 2003; Luo *et al.*, 2003a; 2004; Mould *et al.*, 2003a, 2003b; Barton *et al.*, 2004; Yang *et al.*, 2004a, 2004b).

Because integrin structure is very conserved phylogenetically, invertebrate systems such as *Drosophila melanogaster* provide the opportunity to pursue complementary genetic approaches that are not available in vertebrate organisms (Brower, 2003). We have undertaken a forward genetics strategy in *Drosophila* to identify integrin  $\beta$  subunit mutations that alter integrin function in the context of an intact, developing animal. Here, we report the results of that screen, along with some general inferences that can be drawn from the collection. This includes data from one mutant showing that the screen has generated alleles that can shed light on the structural features that affect integrin functional states.

Article published online ahead of print. Mol. Biol. Cell 10.1091/mbc.E04-02-0085. Article and publication date are available at [www.molbiolcell.org/cgi/doi/10.1091/mbc.E04-02-0085](http://www.molbiolcell.org/cgi/doi/10.1091/mbc.E04-02-0085).

<sup>D</sup> Online version of this article contains supporting material.

Online version is available at [www.molbiolcell.org](http://www.molbiolcell.org).

\* Corresponding author. E-mail address: [dbrower@email.arizona.edu](mailto:dbrower@email.arizona.edu).

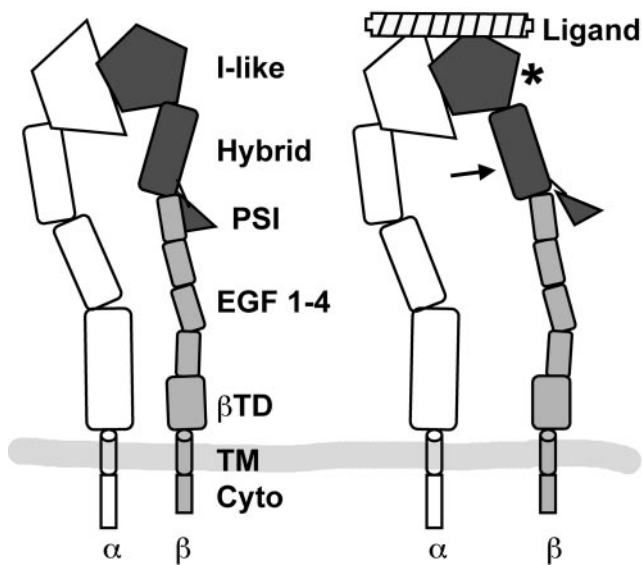


**Figure 1.** Domain structure of integrin heterodimers, in the extended conformation.  $\alpha$  subunit domains are in unshaded outlines. The available data suggest that ligand binding (right) stabilizes an “open” conformation, involving changes in at least two of the three darkly shaded structural domains. In this model, a change in the I-like domain tertiary structure (asterisk) drives a movement of the Hybrid domain; this may also include a dissociation of the PSI domain from a specific binding site on the stalk. EGF 1–4, EGF-like repeats 1–4;  $\beta$ TD,  $\beta$  terminal domain; TM, transmembrane domain; Cyto, cytoplasmic domain.

## MATERIALS AND METHODS

### Mutant Screens

To generate the *mys*<sup>b</sup>- series of alleles, *w*<sup>m</sup> males were mutagenized with ethyl methanesulfonate (EMS; Lewis and Bacher, 1968) and crossed to *CDX*, *y w f* females at 18°C. All marker mutations and special chromosomes are described in Lindsley and Zimm (1992) or in FlyBase (<http://flybase.bio.indiana.edu/>). Because the mothers carried the Compound Double X chromosome, F1 males received their single X chromosome from their mutagenized fathers. Because *mysospheroid* is on the X chromosome, any mutant *mysospheroid* gene must therefore be able to support viability, and so null alleles were eliminated at this point. Individual *w*<sup>m</sup> *mys*<sup>b</sup> F1 males were then crossed to *y mys*<sup>XR04</sup>  *$\beta$ 6a/FM7c* females (*mys*<sup>XR04</sup> is a weak dominant negative allele; Jannuzi *et al.*, 2002), and the F2 progeny were raised at 28°C. If the *mys*<sup>b</sup>/*mys*<sup>XR04</sup> females were dead, the sibling *w*<sup>m</sup> *mys*<sup>b</sup>/*FM7* female and *FM7* male progeny were used to make a balanced stock. The alleles were then retested for lack of complementation with the *mys*<sup>G1</sup> allele, which is similar to *mys*<sup>XR04</sup> but is present in a different genetic background (Jannuzi *et al.*, 2002). *mysospheroid* alleles generated in this way were designated *mys*<sup>b1-b70</sup>.

### Complementation Tests

To score relative viability of various combinations of alleles, eggs were laid at the appropriate temperature, and vials were thinned to prevent overcrowding of larvae. Progeny were scored at least once a day, and if any animals from any single vial were scored, all subsequent progeny from that vial were counted, in order to guard against genotypic differences in developmental rates. In general, newly eclosed animals that were stuck in the food were scored.

### Sequencing of Mutants

Adults or embryos were homogenized and genomic DNA template was isolated according to previously published procedures (Gloor *et al.*, 1993). PCR primers were designed to yield two products covering the *mysospheroid* coding region (exons 2–7; Yee, 1993; Zusman *et al.*, 1993). The first fragment began 139 base pairs before the initiating AUG and the second fragment continued 62 base pairs after the UAG stop codon. The resulting PCR fragments were purified using QIAGEN's QiaQuick PCR Purification Kit (Chatsworth, CA) and sequenced directly by the University of Arizona GATC Automated DNA Sequencing Service. The introns were not sequenced in their entirety.

### Immunofluorescence

For examination of integrin expression levels in situ, all fly cultures were grown at 28°C for at least 2 days before immunostaining. Imaginal discs were dissected from late third instar larvae of the appropriate genotype and stained with the  $\alpha$ PS2 or  $\beta$ PS antibodies CF.2C7 and CF.6G11 as described (Brower *et al.*, 1984). Genotypes included hemizygous *mysospheroid* mutant males or the same with a third chromosome containing both a UAS- $\alpha$ PS2- $\Delta$ CGFFN insert (Baker *et al.*, 2002) and an enhancer trap (337; Manseau *et al.*, 1997) that drives expression of the UAS transgene throughout the imaginal discs. Discs were mounted in VectaShield (Vector Laboratories, Burlingame, CA) and examined using a standard Zeiss immunofluorescence microscope (Thornwood, NY).

For examination of homozygous clones of mutant cells, *mysospheroid* alleles were recombined onto a chromosome with the recombination site *FRT18A*, and females were generated that were heterozygous for this chromosome and an X chromosome also containing *FRT18A* as well as a gene encoding GFP with a nuclear localization sequence, driven by the ubiquitin promoter (Bloomington Stock Center Number 5623). A *hs-FLPase* insert on the second chromosome was induced by several heat shocks during larval life, which led to somatic crossing over at the *FRT18A* sites to produce homozygous *mysospheroid* clones (identified by loss of GFP), and dissected discs were fixed in formaldehyde and stained using the  $\beta$ PS antibody. These discs were photographed using a Nikon E800 confocal microscope (Nikon, Melville, NY).

### Cell Adhesion and Spreading Experiments

*Drosophila* S2/M3 cells transformed with integrin-expressing genes (under the regulation of the heat shock protein 70 promoter) were cultured in Shields and Sang M3 medium supplemented with 12% heat-inactivated fetal calf serum, and  $2 \times 10^{-7}$  M methotrexate for transformed lines (Bunch and Brower, 1992; Zavortink *et al.*, 1993). S2/M3 cells were cotransfected with plasmids expressing the various combinations of wild-type or mutant  $\alpha$ PS2m8 and  $\beta$ PS subunits and the bacterial DHFR selectable marker (Jannuzi *et al.*, 2002). For all experiments, cells were grown in RNAi targeting the endogenous *mysospheroid* gene, as has been described in detail (Jannuzi *et al.*, 2002).

The ligand used in these assays was RBB-Tigg, a bacterial fusion protein that contains 53 amino acids of the *Drosophila* extracellular matrix protein Tigrin (residues 1964–2016, including the RGD sequence and 25 amino acids upstream and downstream), fused to a histidine tag from the pTrcHisB vector (Xpress System, Invitrogen, Carlsbad, CA). This fusion protein is as active in promoting cell spreading as the previously described Tigrin fusion protein and Tigrin itself (Fogerty *et al.*, 1994; T. A. Bunch, unpublished data). The fusion protein was purified by affinity chromatography on Ni-NTA agarose (QIAexpress, QIAGEN). Ninety-six well tissue culture plates or slides were coated with ligand for either 1 h at room temperature or overnight at 4°C, then blocked with 20% dried milk in phosphate-buffered saline (PBS) for 1 h at room temperature, and washed three times with PBS.

Cell spreading assays were done as described (Jannuzi *et al.*, 2002). In brief, cells were treated with dispase/collagenase at 37°C; this heat shock also induces expression of the integrin transgenes. Cells were then allowed to spread in coated 96-well plates for 3–4 h before counting. For adhesion assays, cells were allowed to recover from the protease clearing and heat shock for 4 h, and  $1\text{--}1.5 \times 10^5$  cells in 0.1 ml of M3 medium + 2 mg/ml BSA were added to ligand-coated wells. Cells were allowed to settle and attach for 20 min at 23°C, after which nonadherent cells were removed by washing with a multichannel pipette. The adherent cells were rinsed with PBS and stained with crystal violet (0.5% in 20% methanol) for 1 min. After multiple washes with water to remove unbound dye, the crystal violet was released by the addition of 200  $\mu$ l of 0.1 M citric acid to each well. Dye levels were quantified using an ELX800 Universal Microplate Reader (Bio-Tek Instruments, Burlington, VT) at 562 nm.

For both assays, dose-response curves were done to determine the level of RBB-Tigg that gave maximal cell spreading or adhesion. For the comparisons of wild-type and *mys*<sup>b58</sup>, RBB-Tigg concentrations were selected that gave approximately half-maximal values, in the linear range of the curves. For the spreading assays, RBB-Tigg concentrations were 32 and 8 ng/ml for the wild-type and  $\alpha$ PS2 cytoplasmic mutant integrins; for the adhesion assays, the respective concentrations were 100 and 50 ng/ml. The average and SE from three separate experiments is given. For the adhesion assays, two wells were scored for each data point in each experiment, and background signal from wells not coated with any ligand was subtracted from the values derived from ligand coated wells.

Surface expression levels of  $\alpha$ PS2 $\beta$ PS were checked by flow cytometry for each experiment (Bunch *et al.*, 2004). In all cases, comparisons were made only between pairs of cell lines that expressed similar amounts of integrin, or slightly more wild-type relative to *mys*<sup>b58</sup>.

## RESULTS

### Screen for $\beta$ PS Mutations

To screen for mutations that alter  $\beta$ PS function we made use of the *Drosophila* mutant alleles *mys*<sup>XR04</sup> and *mys*<sup>G1</sup>, which



**Figure 2.** Locations of  $\beta$ PS point mutants. The *Drosophila*  $\beta$ PS and human  $\beta 3$  sequences are aligned, with the locations of  $\beta 3$  structural domains and (for the I-like and hybrid domains) secondary structures indicated (from Xiong *et al.*, 2001). Sites of  $\beta$ PS mutants are underlined with the new residue indicated below, followed by the b-series allele number for mutants generated here, or other allele names for preexisting mutants. Note that *mys*<sup>b70</sup> includes two missense changes. Three alleles involve the insertion of a single residue (*mys*<sup>b50</sup> and *mys*<sup>b62</sup>) or four amino acids (*mys*<sup>b69</sup>) at the splice site indicated by thick underlining between S272 and N273.

make mild dominant negative  $\beta$ PS proteins (Jannuzi *et al.*, 2002). These alleles are fully viable as heterozygotes with wild type, but they typically fail to complement weak alleles of *myospheroid*. This property allows one to design a screen to identify mutations that compromise  $\beta$ PS function without eliminating it (see MATERIALS AND METHODS). In this screen, the mutant *myospheroid* gene must retain sufficient  $\beta$ PS activity to permit the survival of an F1 male (*myospheroid* is on the X chromosome) after EMS treatment. The mutant is then tested for lethality when combined with a weak dominant negative allele of *myospheroid*. Still, we find that some relatively strong alleles have been recovered, probably because after EMS mutagenesis the F1 males can be genetically mosaic for the *myospheroid* mutation (Ashburner, 1989). Indeed, for three alleles (*mys*<sup>b23</sup>, *mys*<sup>b26</sup>, and *mys*<sup>b64</sup>) we have not seen a mutant male since the original F1 animal; each of these mutant X chromosomes can be rescued by the small *mys*<sup>+</sup> duplication *Tp(1;2)sn<sup>+</sup>72d*, indicating that the lethality is not due to a mutation at another locus.

**Point Mutations in  $\beta$ PS**

We sequenced the coding exons and nearby splice sites for all of the new mutants from this screen as well as a number

of *myospheroid* alleles from previous screens. Alleles generated in our screen are designated *mys*<sup>b</sup>; other alleles associated with point mutations in the coding region that retain some function include *mys*<sup>ts2</sup> (Wright, 1968) and *mys*<sup>XN101</sup> (Wieschaus *et al.*, 1984). In all, we identified  $\beta$ PS point mutations in 55 hypomorphic or neomorphic alleles, which comprised 49 different molecular lesions. Included in our definition of “point” mutations are three alleles that insert one or four residues at the splice site between exons 4 and 5. Additionally, we previously described two missense alleles (*mys*<sup>G4</sup> and *mys*<sup>G12</sup>) from another screen that have phenotypes similar to the null phenotype (Jannuzi *et al.*, 2002).

We failed to find molecular lesions in seven alleles, including *mys*<sup>b5</sup>, *mys*<sup>b8</sup>, *mys*<sup>b9</sup>, and *mys*<sup>b36</sup> from this screen, *mys*<sup>ts1</sup> and *mys*<sup>ts3</sup> (Wright, 1968) and *mys*<sup>nj42</sup> (Costello and Thomas, 1981). In all but *mys*<sup>b36</sup> (which was not mapped) the mutation has been mapped genetically to a small chromosomal region that includes *myospheroid*, and in some cases defects in  $\beta$ PS expression have been detected (unpublished data). Thus, we assume that these represent regulatory mutations.

Figure 2 shows the predicted  $\beta$ PS amino acid changes for all of the identified *myospheroid* point mutants (see Supple-

mentary Information for a compilation of nucleotide changes). The sequences of integrin  $\beta$  subunits indicate that the overall structures of the proteins are strongly conserved, and the sites of almost all of the  $\beta$ PS changes can be easily matched to corresponding residues in human  $\beta$ 3, for which there are x-ray structural data for most of the extracellular region (Xiong *et al.*, 2001). We will use these correspondences as well as other data from human integrins, in making structural inferences below.

Not surprisingly, the distribution of the mutations is not uniform throughout the protein. In the I-like domain, ~10% of the residues were mutated, whereas the hybrid domain was the least sensitive structure, with only 1% of the residues hit. The PSI domain and stalk region showed intermediate sensitivity, with 6–7% of the amino acids in each being mutated.

### Genetic Characterizations

For most of the alleles we tested viability in a variety of genetic combinations, including as hemizygous males, as heterozygotes over a *myospheroid* null allele or the original dominant negative allele, and finally as heterozygotes over a *myospheroid* null in addition to being heterozygous for *mew* (encoding  $\alpha$ PS1) or *inflated* ( $\alpha$ PS2). (A number of the strong alleles were not tested in this way, because of the very low viability of the mutant males.) These tests were carried out at a range of temperatures from 18°C to 28°C, because *myospheroid* hypomorphs generally display stronger phenotypes (including lethality) at higher temperatures (Bunch *et al.*, 1992). For strong alleles failure to complement the dominant negatives is usually complete at all temperatures, although our alleles alone or over the null allele are often viable, especially at low temperatures. Alleles designated as “weak” typically complement the dominant negative mutant at low temperatures. Heterozygosity for  $\alpha$ PS alleles increases lethality of the  $\beta$ PS hemizygotes; this is especially true for  $\alpha$ PS2. We do not see any extreme examples of  $\alpha$  subunit specificity in viability reduction for particular  $\beta$ PS alleles, although weak trends could be detected for some. These viability tests were used to define alleles as strong, moderate or weak in Table 1 (see Supplementary Information for details).

In a previous small scale examination of three *myospheroid* hypomorphs, it was not possible to identify a discrete lethal phase or phenotype (T. Wright, personal communication). Although we have not made a comprehensive examination of all of our mutants, we also see that under conditions in which they are lethal, many of our alleles do not show well-defined phenotypes or stages of lethality. However, it does appear that embryonic development is more sensitive than most stages. For example, viability can often be enhanced significantly if animals are allowed to traverse embryogenesis at a relatively low temperature, which ameliorates the effects of integrin hypomorphs generally.

Discrete adult phenotypes also are not common for the *myospheroid* alleles. Some mutants can display the held-out wing phenotype that has been described previously (Wilcox, 1990), depending on temperature or genetic background, but this is not usually found in hemizygotes at low temperature, for example. Wing blisters, a clonal phenotype of null *myospheroid* alleles (Brower and Jaffe, 1989), are extremely rare in viable animals, with one notable exception described below. We generated clones of homozygous mutant cells via somatic recombination (Xu and Rubin, 1993) for a number of the point mutants (see Table 1). In addition to the strong alleles *mys<sup>G4</sup>* and *mys<sup>G12</sup>*, which were originally identified based on this clonal wing blistering phenotype (Jannuzi *et*

*al.*, 2002), only *mys<sup>b23</sup>* and *mys<sup>XN101</sup>* produce wing blisters in clones. Both *mys<sup>b23</sup>* and *mys<sup>XN101</sup>* also show 100% embryonic lethality.

### Integrin Expression in Imaginal Discs

Because we are especially interested in mutations that affect function but not expression, many of the alleles were tested for cell surface integrin levels in third instar wing imaginal discs *in situ*. In all cases we examined discs grown at 28°C, when mutant phenotypes are expected to be strongest (although typically the animals were allowed to traverse the sensitive embryonic period at lower temperatures to increase viability). We also examined expression in wing discs that ubiquitously expressed an  $\alpha$ PS2 subunit containing an activating cytoplasmic mutation (deletion of the CGFFN sequence; O’Toole *et al.*, 1994). This mutation leads to reduced heterodimer expression, and constitutive clustering on the basal surface of the disk cells (Baker *et al.*, 2002). Because  $\alpha$ PS2 is normally expressed only on the cells that will give rise to the ventral wing surface at this stage, staining these wing discs with an antibody against  $\alpha$ PS2 allows one to compare expression of the  $\beta$ PS allele with wild-type  $\alpha$ PS2, on the presumptive ventral epithelium, and activated  $\alpha$ PS2 specifically on the dorsal side of the same disk (Figure 3). Not all alleles were tested for expression, in part because some were difficult to grow as hemizygotes under the conditions of the experiment. However, for some of the latter alleles expression was examined in clones of homozygous mutant cells of the wing disk epithelium (Figure 4); these clones were generated by somatic recombination in developing heterozygotes (Xu and Rubin, 1993).

As summarized in Table 1, most *myospheroid* hypomorphs are expressed well in discs, suggesting that general destabilization of the heterodimers cannot account for the loss of viability in the screen. However, especially for the I-like domain alleles, heterodimers with a  $\beta$ PS mutation and the activating  $\alpha$ PS2 alteration are often present at much lower levels, and in many cases these are virtually undetectable on the dorsal epithelium. To ask if the I-like domain point mutants cluster into any particular part of the structure, we mapped our alleles onto the x-ray trace of the human  $\beta$ 3 subunit (Figure 5). There is no suggestion that a particular region of the I-like domain, such as the cation binding sites or the  $\alpha/\beta$  interface, is especially sensitive to this type of destabilizing mutation. Alleles are found in all parts of the domain, and the collection includes residues with side chains either on the external surface or the interior of the structure (including some that simply replace an internal hydrophobic residue with a larger hydrophobic amino acid).

Decreased expression of activated heterodimers is not typically found for mutations in the stalk region. However, in a reversal of the I-like domain trend, a mutant (*mys<sup>b60</sup>*) at the boundary between the second and third EGF-like repeats (E600>K) shows reduced expression normally in discs, but is expressed at least as well as wild-type  $\beta$ PS when paired with the activated  $\alpha$ PS2 subunits. Because this result was unusual, we confirmed the decreased expression with the wild-type  $\alpha$ PS2 by making clones of homozygous *mys<sup>b60</sup>* cells in a heterozygous background, where the difference in expression is clearly evident at the clone boundary (Figure 4). This region of the  $\beta$  stalk is not resolved in the x-ray structures, and probably undergoes significant changes when the heterodimer switches from the bent to extended conformations. The glutamate that is mutated in *mys<sup>b60</sup>* is well conserved in  $\beta$  subunits, and our data suggest that this residue is likely to make specific interactions that stabilize the inactive conformation. These data are also consistent

Table 1. Summary of  $\beta$ PS point mutants

Allele	Change	Location	Strength	Expression	
				Wild type $\alpha$	Activated $\alpha$
b41	C40Y	PSI	Strong	OK (c)	
b33	I50F	PSI	Weak	OK-c	
b3	C58S	PSI	Moderate	OK	Reduced
b68	C58Y	PSI	Strong	Reduced (c)	Much reduced
G4	S196F	cation coord	Lethal		
b67	D200N	cation coord	Strong	OK-c	
b38, b61	L224F	Interior	Weak	OK	OK
b26	G227S	Interior	Strong	OK-c	
b20, b59	P242L	$\alpha/\beta$ interface	Weak	OK	OK
b21	L264F	Interior	Strong	OK-c	Gone
b50, b62	272+Q	Insertion	Weak	OK	Reduced
b69	272+SVRQ	Insertion	Strong	OK	Gone
b13	E274V	Surface	Strong	OK-c	
b47	A293T	Interior	Strong	OK	Gone
b30	I298F	Interior	Strong	OK	Much reduced
b65	A310T	Interior	Weak	OK	Much reduced
b45	R312Q	Interior	Moderate	OK	
b25	S317L	Interior	Weak	OK	OK
b48	A325T	$\alpha/\beta$ interface	Strong	OK	Gone
b66	P336S	$\alpha/\beta$ interface	Strong		
b57	G339S	Interior	Strong	OK	Gone
b49	H342Y	Interior	Weak	OK	
ts2	G347D	Surface	Weak	OK	
b42, b43	G347S	Surface	Weak	OK	Much reduced
G12	D356N	$\alpha/\beta$ interface	Lethal		
b44	I375F	Interior	Moderate	OK	
b53	E387V	Surface	Weak	OK	
b56	G395S	Surface	Strong	Reduced	Reduced
b7	D404N	Surface	Weak	OK	
b23	N407Y	Surface	Strong	OK-c	
b58	V409D	"Surface"	Weak	OK-c	
b27	V423E	Hybrid	Strong	OK	Gone
b37	C441Y	Hybrid	Weak	OK	OK
b63	G531D	EGF-1	Weak	OK	OK
b31	G541S	EGF-1	Weak	OK	OK
b64	C544Y	EGF-1	Strong	Reduced-c	
b55	R587Q	EGF-2	Weak	OK	
b46	G596S	EGF-2	Weak	OK	
b52	G596R	EGF-2	Strong	OK	
b24, b28, b60	E600K	EGF-3	Weak	Reduced (c)	OK
b51	E607K	EGF-3	Strong	Reduced (c)	
XN101	C629S	EGF-3	Strong	OK-c	
b22	R676C	EGF-4	Weak		
b39	G679D	EGF-4	Weak	OK	
b4	C701Y	$\beta$ TD	Weak	OK	
b34	G707S	$\beta$ TD	Weak	OK	OK
b29	F743I	$\beta$ TD	Weak	OK	OK
b32	V763M	$\beta$ TD	Weak	OK	OK
b40	V775D	$\beta$ TD	Weak	OK	OK
b1	G792D	Transmem	Moderate	OK	OK
b70	S836T, P841T	Cytoplasm	Strong	OK (c)	OK

Allele "strength" is based on viability in various genetic tests (see text and Supplementary Information). Expression of "inactive" and "activated" proteins refers to surface protein on third instar wing imaginal disc cells with wild-type  $\alpha$ PS2 subunits or  $\alpha$ PS2 with a cytoplasmic CGFFN deletion. Those indicated as "-c" were determined in clones of homozygous mutant cells in the disc epithelium; those with "(c)" were scored in whole discs as well as clones. "Location" indicates the  $\beta$  domain or, for the I-like domain, the location of the the residue side chain; cation-coordinating,  $\alpha/\beta$  interface, etc corresponds to the color coding of mutants in Figure 5. *mys*<sup>b21</sup> is in the alternatively spliced fourth exon and is specific to the predominant 4A  $\beta$ PS isoform. Note that *mys*<sup>b50</sup>, *mys*<sup>b62</sup>, and *mys*<sup>b69</sup> are insertions after residue 272, resulting from changes in splicing. The identity of these mRNAs has been confirmed by RT-PCR, and no wild-type mRNA was detected (unpublished data). *mys*<sup>b70</sup> changes two nearby residues in the cytoplasmic tail. The *mys*<sup>b</sup> series alleles were generated in this screen; the null-like *mys*<sup>G4</sup> and *mys*<sup>G12</sup> alleles are from a screen for strong integrin mutants (Jannuzzi *et al.*, 2002); *mys*<sup>ts2</sup> is from a screen for hypomorphs by Wright (1968). *mys*<sup>XN101</sup>, from the screens of Wieschaus *et al.* (1984), is 100% lethal but retains some *mys*<sup>+</sup> activity, based on the embryonic lethal phenotype.

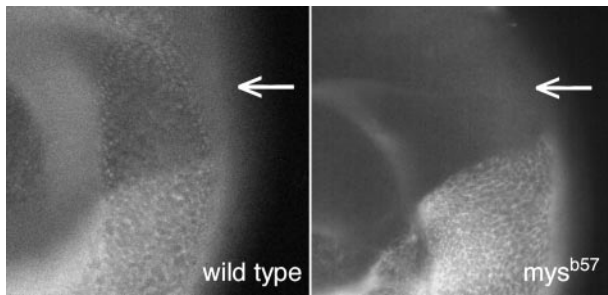


**Figure 3.** Expression of  $\alpha$ PS2 $\beta$ PS integrins in the posterior margin of third instar larval wing imaginal discs. Typically,  $\alpha$ PS2 $\beta$ PS is expressed only in the ventral (lower) half of the epithelium, but these animals are also expressing a transgenic  $\alpha$ PS2 subunit with a cytoplasmic activating mutation (deletion of CGFFN) throughout the disk. The upper staining (arrows) is entirely from the transgenic activated  $\alpha$ PS2 with  $\beta$ PS, whereas the lower immunostaining is primarily from wild-type  $\alpha$ PS2 with  $\beta$ PS, which is much more stable than heterodimers containing the activating  $\alpha$ PS2 mutation. For wild-type  $\beta$ PS, the dorsal staining is reduced relative to the ventral staining, and the activated heterodimers are clustered on each cell. For many  $\beta$ PS mutants, expression with the activated  $\alpha$ PS2 subunits is reduced much more than for wild-type, or is even nondetectable, as shown here for *mys*<sup>b57</sup>. See Table 1 for a summary of the imaginal disk expression data.

with recent findings that disruption of the disulfides immediately surrounding the *mys*<sup>b60</sup> residue promote integrin activation (Kamata *et al.*, 2004).

#### *mys*<sup>b58</sup> Is a Gain of Function Allele

The allele *mys*<sup>b58</sup> is unusual in that in various combinations with other integrin mutants it causes a high frequency of wing blisters. Blisters are especially common when *mys*<sup>b58</sup> animals are also heterozygous for  $\alpha$ PS mutations. Typically, wing blisters are created when patches of cells in the wing epithelium are homozygous for strong loss-of-function mutations in *myospheroid* (Brower and Jaffe, 1989). Blisters may also be seen in PS integrin regulatory alleles (e.g., Bloor and Brown, 1998), but they are rarely seen in the  $\beta$ PS point mutant hypomorphs, probably because these alleles alter integrin function more globally, and the level of function necessary to hold the wing epithelia together is less than that required for one or more essential events during development. Paradoxically, even though *mys*<sup>b58</sup> causes a relatively strong wing phenotype, it is a very weak allele by all of the genetic tests for viability. One model that might explain this paradox is that *mys*<sup>b58</sup> may promote integrin activation. For example, gain-of-function  $\alpha$ PS2 mutations, if inappropriately expressed in developing wings, promote wing blistering (Baker *et al.*, 2002).

The screen was not necessarily designed to uncover integrin gain-of-function alleles, and so we decided to further assess the properties of *mys*<sup>b58</sup> more directly in cell culture. Only one nucleotide alteration was found in the coding region of *mys*<sup>b58</sup> (T1226>A, where nucleotide 1 is the A of the initial AUG), which would lead to a single amino acid change (V409>D). We expressed  $\beta$ PS subunits containing the V409>D mutation along with  $\alpha$ PS2 in *Drosophila* S2 cells and compared the activity of this mutant with wild-type  $\beta$ PS in two assays. Adhesion was measured by allowing cells to settle onto a substratum coated with a fragment of the  $\alpha$ PS2 $\beta$ PS ligand Tigrin (RBB-Tigg), followed by removal of nonadherent cells by washing 20 min later. Cell spreading was assessed by direct observation at 3–4 h after plating. In both assays, the *mys*<sup>b58</sup> mutant cells show increased activity relative to those expressing wild-type  $\beta$ PS (Figure 6).

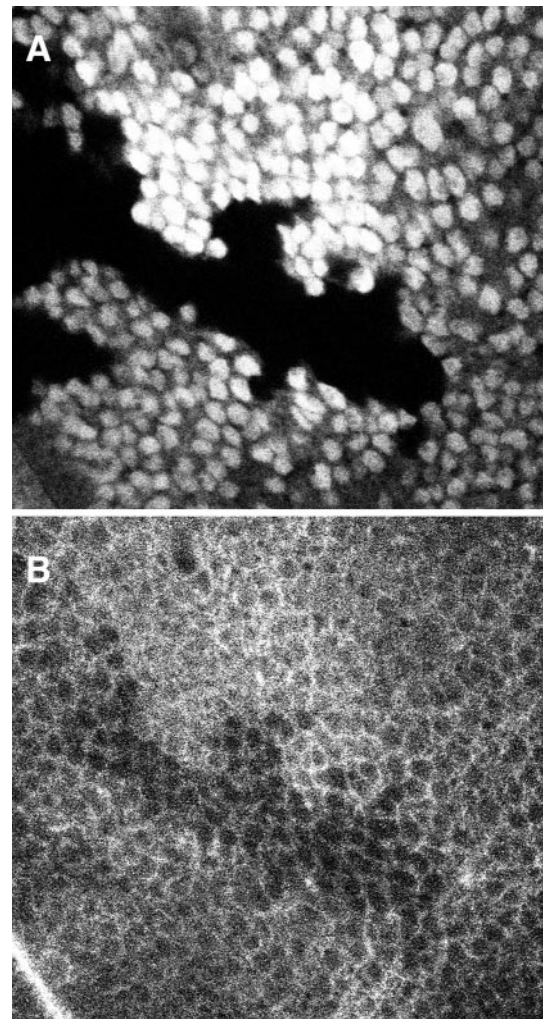


**Figure 4.** Examination of integrin surface expression via clonal analysis. A clone of cells homozygous for *mys*<sup>b60</sup> was generated in a heterozygous *mys*<sup>b60</sup>/*mys*<sup>+</sup> background, by somatic recombination in a cell of the early wing imaginal disk epithelium. The clone is marked by the loss of nuclear GFP staining (A), which derives from a transgene on the *mys*<sup>+</sup> chromosome. The homozygous *mys*<sup>b60</sup> cells show reduced surface integrin expression, as indicated by staining for  $\beta$ PS (B).

S2 cells expressing integrins with an  $\alpha$ PS2 subunit containing an activating cytoplasmic mutation (GFFNR>GFANA) adhere and spread extraordinarily well under similar conditions even though integrin expression is typically reduced. Combining *mys*<sup>b58</sup> with activating  $\alpha$ PS2 subunits results in even greater adhesion and spreading ability than is seen for the cytoplasmic mutation alone (Figure 6), and the difference attributable to *mys*<sup>b58</sup> is similar to that seen with wild-type  $\alpha$ PS2. This suggests that these two mutations are affecting different factors that alter integrin function in these assays; this is discussed more fully below. Finally, the data presented in Figure 6 were generated using the “m8” isoform of  $\alpha$ PS2 (Brown *et al.*, 1989); preliminary experiments indicate that *mys*<sup>b58</sup> also enhances the activity of heterodimers containing the “c” isoform of  $\alpha$ PS2.

## DISCUSSION

The results of this screen indicate that forward genetics can provide an important complement to site-directed mutagen-

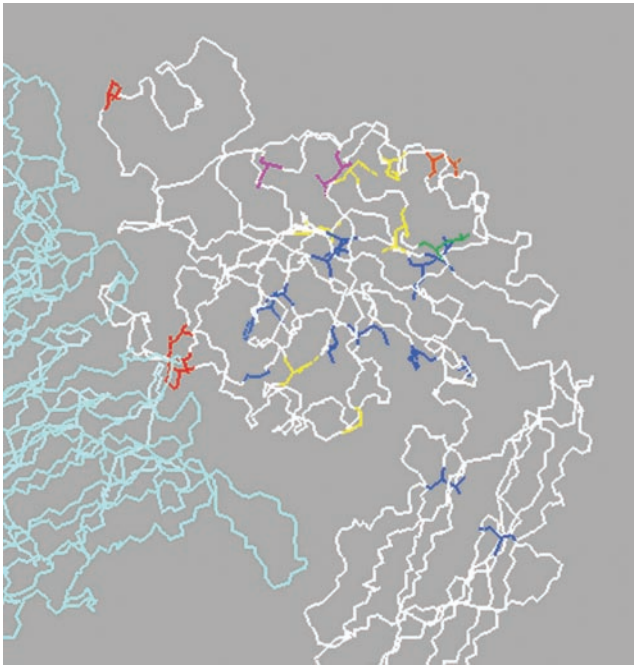


**Figure 5.** Locations of I-like domain and hybrid domain  $\beta$ PS mutants, mapped onto the structure of  $\alpha$ v(pale blue) $\beta$ 3(white). Categories of mutations are:  $\alpha/\beta$  interface-red; side chain on surface-yellow; side chain on interior-blue; side chain that coordinates with cation-purple; location of insertions-orange;  $mys^{b58}$ -green (see below). There is no obvious hyper-sensitive region for I-like domain mutants.

esis for understanding complex molecular dynamics of proteins. Moreover, the scale of this mutagenic screen is such that one can begin to draw inferences based on the overall distributions of the mutants. For example, it appears that our mutations are more common in regions that are molecularly dynamic. The I-like domain, which is thought to undergo extensive tertiary structural changes, was hit most frequently (10% of all residues in the domain), whereas the neighboring hybrid domain, which is likely to function as a more solid unit, was relatively untouched (1%). The surprising number of mutations in the stalk suggests that individual domains within this region also undergo significant structural rearrangements during conformational switching; this is in keeping with the unstructured state of much of the stalk in the  $\alpha$ v $\beta$ 3 crystal (Xiong *et al.*, 2001; see also Beglova *et al.*, 2002).

The analysis of the  $mys^{b58}$  allele begs the question as to why a screen that is designed to uncover integrin loss-of-function mutations would also yield gain-of-function alleles. Proper regulation of function is essential for many integrin mediated events, and it has been documented that strongly hyperactive integrins will not necessarily support wild-type morphogenesis (or viability) of developing *Drosophila* (Martin-Bermudo *et al.*, 1998). Furthermore, the screen selects for mutants that are lethal over an allele ( $mys^{XR04}$ ) that has defects in regulation (Jannuzi *et al.*, 2002), probably including both inside-out and outside-in signaling (B. James, unpublished results). Thus, in retrospect it is not surprising that the screen can yield mutants that affect integrin function in relatively complex and unpredictable ways. Indeed, this is one of the main advantages of forward genetic approaches and especially of screens conducted in whole animals, where the full range of integrin functions required in various tissues will be sampled.

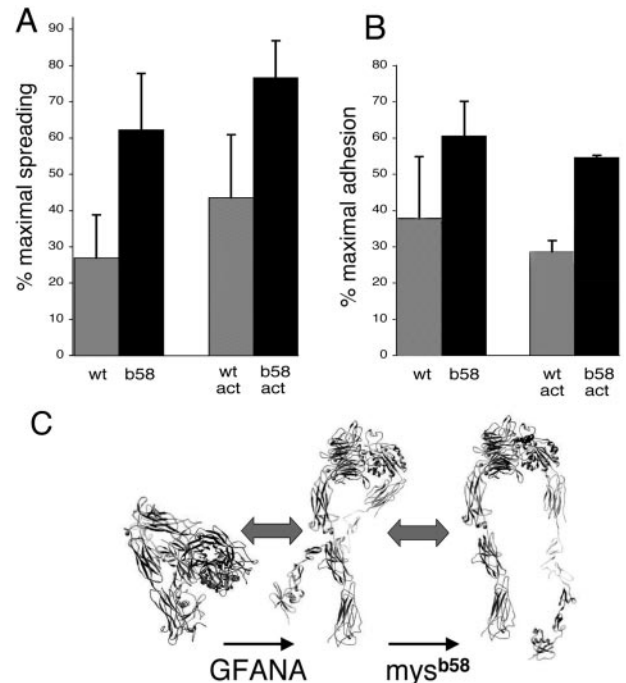


**Figure 6.** (A and B) Spreading and adhesion of S2 cells expressing  $\alpha$ PS2 and wild-type or  $mys^{b58}$  (V409>D)  $\beta$ PS. Cells were allowed to settle on plates coated with an RGD-containing fragment of the *Drosophila* ECM protein Tigrin (RBB-Tigg). Spread cells (A) were defined by phase microscopy 3–4 h after plating. Adhesion (B) was defined by the number of cells remaining attached after washing 20 min after settling onto the plate. Ligand concentrations were chosen that give approximately half-maximal spreading or adhesion for each pair of bars (see MATERIALS AND METHODS), and the values are expressed as a percentage of the maximum at high RBB-Tigg concentrations; this adjusts for variations in expression or other factors between experiments. For the right pairs of bars in each histogram (labeled “act”),  $\beta$ PS was combined with  $\alpha$ PS2 subunits containing a cytoplasmic-activating mutation (GFFNR>GFANA). In each pairwise comparison, spreading is significantly increased for the  $mys^{b58}$  allele compared with wild-type  $\beta$ PS, and the amount of the increase is approximately the same whether  $\beta$ PS is paired with wild-type or cytoplasmically activated  $\alpha$ PS2. (C) These data are most easily explained by a two-stage model of integrin activation, in which the equilibrium between bent and extended heterodimers is regulated primarily by cellular events, and the equilibrium between the open and closed conformations of the integrin head is affected by  $mys^{b58}$  (protein tracings from Shimaoka and Springer, 2003). Data are averages from three experiments, and integrin expression levels in each case were generally similar or slightly higher for the wild-type  $\beta$ PS cells (unpublished data).

A recent study of cysteine mutants in the EGF-like repeats of the  $\beta$ 3 stalk suggests that this region is important for the maintenance of inactive conformations (Kamata *et al.*, 2004), and so we might expect that some of our alleles in this region will show more complex effects than simple reduction of integrin function. Comparisons between this study of  $\alpha$ IIb $\beta$ 3 and our screen point out again the complementary nature of data from cell culture and whole animals. For example, mutation C549>S of  $\beta$ 3 gave the highest “activation index” measured by Kamata *et al.* (2004); mutation of the homologous residue in flies (C629>S) is 100% embryonic lethal in hemizygous males. Mutation of a PSI domain cysteine (C26>S) in  $\alpha$ IIb $\beta$ 3-expressing cells had little effect on fibrinogen binding and activation index; the homologous change in  $\beta$ PS ( $mys^{b3}$ ) leads to increased integrin activity in S2 cells (T. A. Bunch, unpublished results) but temperature-

sensitive lethality in developing animals. Finally, the available data suggest that disruption of the long range disulfide connecting the PSI domain and stalk should be very strongly activating (Sun *et al.*, 2002), and one might expect this change to disrupt integrin regulation sufficiently to be lethal in embryos. Although elimination of this disulfide in *mys<sup>b41</sup>* is a relatively strong allele, fertile adults can be obtained, and expression of the heterodimers in imaginal discs is not significantly affected.

Another feature of an unbiased genetic screen is that one routinely samples alterations that may do something other than just eliminate a functional side group. For example, the *mys<sup>b67</sup>* mutation changes a conserved aspartate that coordinates with the ADMIDAS cation that appears to direct I-like domain movements (Xiong *et al.*, 2001, 2002; Chen *et al.*, 2003; Mould *et al.*, 2003b). This residue might be expected to be critical for integrin function in at least one developmental context and therefore be 100% lethal; however, *mys<sup>b67</sup>* routinely retains enough activity to support embryonic development through hatching into first instar larvae (well beyond the stage when null alleles die) and even can produce very rare viable adults. This could be because the asparagine that replaces the aspartate in *mys<sup>b67</sup>* may not completely eliminate the ADMIDAS site function. In three other sites, the screen yielded mutations in the same residue that have different severity, depending on the nature of the change (Table 1).

Of course, because of the starting wild-type nucleotide sequence and the chemical nature of the mutagenesis, any residue is likely to be converted into only a subset of the 20 possible amino acids. However, numerous alternatives may be tested in a random EMS mutagenesis. Although G-to-A transitions are the most common mutations created by EMS, other alterations are not particularly rare. Indeed, of the missense alleles we have sequenced, 29% are caused by a nucleotide change other than G-to-A. Moreover, once a critical site has been identified by one mutation, additional changes can subsequently be sampled by more directed methods.

#### Requirements for Specific Amino Acids in Integrin $\beta$ Subunits

The overall structure of integrins is strongly conserved, probably because of the intricate interactions between and within  $\alpha$  and  $\beta$  subunits during the various conformational changes of the heterodimer, and the majority of our mutations are in residues that are at least similar in most  $\beta$  subunits. Phylogenetically conserved residues are most likely to be important for protein function, and so it is not surprising that changing these will have noticeable effects. However, it is remarkable that so many strongly conserved amino acids can be altered without preventing morphogenesis in all of the mutant flies. Of the mutants generated here, only *mys<sup>b23</sup>* has an embryonic lethal phenotype that is somewhat similar to that of a null allele. Four alleles eliminate completely conserved cysteines but retain some adult viability. Four other alleles change residues that are 100% conserved in all of the 25  $\beta$  subunits sequenced to date, and either produce some adults or reliably develop through embryogenesis and hatch as larvae. And 14 alleles that give adult animals are in residues that are conserved in 20 or more  $\beta$ s. (A number of these latter are conserved in all except some of the very divergent  $\beta$  subunits, such as  $\beta 8$  or the insect  $\beta v$ .) Not included in this group are more mutations that change the nature of residues that are similar in virtually all  $\beta$ s, such as small hydrophobic amino acids.

Although missense alleles with altered function were fairly easy to obtain in this screen, we previously noted that missense alleles were relatively rare among the strong *myspheroid* mutants generated by EMS mutagenesis, which is expected to produce point mutations primarily (Jannuzi *et al.*, 2002). Indeed, splice site mutants were more common than missense mutations, suggesting that relatively few residues of  $\beta$ PS are absolutely required for integrin function, even in the context of a whole, developing animal. Taken together, the data from these screens indicate strongly that most integrin functions are driven by a set of relatively weak molecular interactions and that few contributing residues are absolutely essential.

The cytoplasmic domain is unusual in that it contains a high frequency of well conserved residues but yielded only one mutation in this screen. There are a number of possible reasons for this discordance, including the fact that the small size of this region (45–50 residues) weakens the statistical significance of the correlation. However, one possible explanation for the paucity of cytoplasmic alleles is that a relatively high percentage of the conserved residues in this domain are required in order to attain the level of integrin function required for passage of the mutagenized males through the F1 generation of the screen. It may be significant that many conserved cytoplasmic amino acids appear to contribute to specific interactions with other proteins (Liu *et al.*, 2000), whereas most of the conserved extracellular residues are involved in integrin heterodimer structure-function. Interestingly, the one cytoplasmic allele we did find, *mys<sup>b70</sup>*, specifically (compared with two extracellular *myspheroid* hypomorphs) displays strong genetic interactions with mutations in the cytoplasmic integrin-binding protein talin (unpublished data).

#### Stability of Activated Heterodimers

We find that many of our  $\beta$  I-like domain mutants have dramatic effects on integrin expression only when paired with activating  $\alpha$ PS2 subunits. One possibility is that all of these alleles disrupt interactions that are specific to one tertiary state of the I-like domain, but it seems unlikely that we could be so fortunate as to uncover such a high percentage of mutations with such specificity. A more plausible scenario is that most of these alleles make the  $\beta$  subunit slightly less stable, but in the inactive (in this case, probably bent) conformation the heterodimer is held together by an excess of molecular interactions. However, if forced into an upright conformation, the mutant heterodimers may lack sufficient stability to persist, especially in the absence of potentially stabilizing integrin-ligand interactions (Luo *et al.*, 2003b). Consistent with this interpretation, a number of mutants were found that might be expected to “loosen up” the tertiary structure of the I-like domain, for example, by replacing an internal hydrophobic residue with a larger hydrophobic amino acid. In general, these did not significantly affect heterodimer expression levels when paired with wild-type  $\alpha$ PS2 in imaginal discs, although they could reduce expression of the mutationally activated integrins.

$\alpha$  subunit cytoplasmic activating mutations often result in decreased expression, and it is not known if this is because of rapid turnover, inability to reach the cell surface, or both. We do not know which events are affected in our cells either, but wherever the instability occurs, the I-like domain mutants appear to be lowering the permissible baseline and demonstrate clearly that constitutive cytoplasmic activation does indeed decrease heterodimer stability. Our data do not directly address the issue of whether activation per se leads to a separation of the  $\alpha$  and  $\beta$  heads, as has been suggested



(Hantgan *et al.*, 1999, 2001; see also Luo *et al.*, 2003b). Most probably, observed separations seen in isolated heterodimers depend on the conditions of preparation and are not typical of integrins in cellular membranes, but in any case these structures are indicative of reduced stability that would be expected to be augmented by the destabilizing effects of I-like domain mutations.

#### *mys*<sup>b58</sup> and Integrin “Activation”

The cell adhesion and spreading assays support the idea that the unusual wing blistering phenotype of *mys*<sup>b58</sup> is actually due to a gain-of-integrin function. These assays were performed with a Tiggrin fragment. Because Tiggrin is not critical in wing morphogenesis (Bunch *et al.*, 1998), it remains a formal possibility that *mys*<sup>b58</sup> affects binding to a wing ligand specifically, although from the available structural data there is no reason to suspect that residue V409 would affect ligand-specific functions. Preliminary experiments indicate that *mys*<sup>b58</sup>-expressing cells function at least as well as cells expressing wild-type  $\beta$ PS on a fragment of an RGD-containing protein that is likely to serve as an integrin ligand in the wing, Wingblister-laminin (Graner *et al.*, 1998; Martin *et al.*, 1999).

In addition to the domains conserved in essentially all integrins, a number of integrins contain a ligand-binding I domain (also known as the A domain) attached to their  $\alpha$  subunits, and for a few of these I domains x-ray and other experimental data exist for both the open (ligand binding) and closed conformations. Opening of the I domain causes a downward extension of the C terminal  $\alpha 7$  helix (Lee *et al.*, 1995; Emsley *et al.*, 2000), and conversely, mutagenesis experiments have shown that promoting this movement can increase I domain ligand binding (Xiong *et al.*, 2000; Lu *et al.*, 2001; Yang *et al.*, 2004b).

By analogy with  $\alpha$  subunit I domains, it has been proposed that upon complete activation the  $\alpha 7$  helix of the integrin  $\beta$  subunit I-like domain moves down, causing the observed pivoting of the hybrid domain out away from the  $\alpha$  subunit (Takagi *et al.*, 2002; Liddington and Ginsberg, 2002; Luo *et al.*, 2003a). In support of this idea, mutation of a conserved hydrophobic residue at the base of the  $\alpha 7$  helix has been demonstrated to promote the exposure of activation epitopes in the hybrid domain (Mould *et al.*, 2003a). Most convincingly, Luo *et al.* (2004) have recently demonstrated that locking the  $\alpha 7$  helix of  $\beta 3$  in different positions with disulfides has the predicted consequences on heterodimer affinity states, assuming that this structure functions similarly to the homologous helix of  $\alpha$  subunit I domains. Moreover, deletion of one turn of the I-like domain  $\alpha 7$  helix has been tied to shape changes which increase ligand binding affinities at the distal end of the domain (Yang *et al.*, 2004a).

The *mys*<sup>b58</sup> mutation alters a residue ( $\beta$ PS V409) which, by homology to  $\beta 3$ , sits near the top of the  $\alpha 7$  helix of the I-like domain. This residue is hydrophobic in 24 of the 25 integrin  $\beta$  subunits sequenced to date, and in the original x-ray structure of  $\alpha v\beta 3$  (Xiong *et al.*, 2001) the closest side chain neighbors to the residue homologous to  $\beta$ PS V409 ( $\beta 3$  L341) are two conserved hydrophobic residues of the  $\alpha 1'$  helix. *mys*<sup>b58</sup> inserts an aspartic acid residue into this hydrophobic interface and would be expected to disrupt the association between these structures. Indeed, in the x-ray structure of  $\alpha v\beta 3$  in combination with an RGD peptide ligand (Xiong *et al.*, 2002) the top of the  $\alpha 7$  helix dissolves and  $\beta 3$  L341 (homologous to  $\beta$ PS V409) is rotated away from the  $\alpha 1'$  helix, becoming exposed on the exterior of the I-like domain (Figure 7). Previous data have indicated that ligand binding

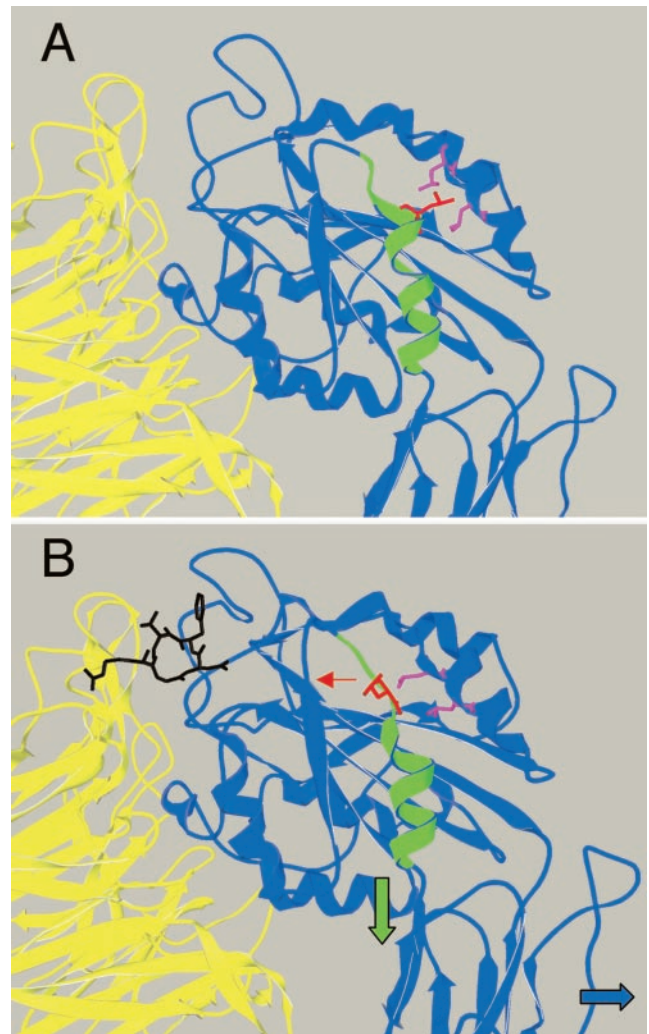


**Figure 7.** Structural basis for the activating effects of *mys*<sup>b58</sup>. The movement of the  $\beta 3$  residue (L341) homologous to  $\beta$ PS V409, in the unliganded I-like domain (A) and in similar crystals infused with a peptide ligand (B) (structures from Xiong *et al.*, 2001, 2002). In the “liganded” structure, the L341 side chain (red) rotates away from the neighboring hydrophobic side chains of the  $\alpha 1'$  helix (purple), toward the solvent. This would facilitate a proposed downward movement of the  $\alpha 7$  helix (green) and the rightward rotation of the hybrid domain (blue arrow), although these latter movements are not seen in these crystals, which are still in the “bent” conformation (see Figure 6).

induces movements of the  $\alpha 1$ - $\alpha 1'$  helices (Xiong *et al.*, 2002; Mould *et al.*, 2002), and the data from *mys*<sup>b58</sup> point to mechanisms whereby this change could be coordinated with movements of the  $\alpha 7$  helix (Luo *et al.*, 2004).

Although there is no significant downward movement of the  $\alpha 7$  helix in the  $\alpha v\beta 3$ -RGD peptide x-ray structure (Xiong *et al.*, 2002), this is likely due to constraints imposed on the bent conformation of the integrins in the crystal lattice. The increase in activity seen for *mys*<sup>b58</sup> even in the presence of a strongly activating cytoplasmic  $\alpha$  subunit is most easily explained by a two-stage model of integrin activation (Takagi *et al.*, 2002; Figure 6C), in which the *mys*<sup>b58</sup> mutation preferentially promotes structural changes after the transition to the upright conformation. In this regard, it is noteworthy that artificially locking the  $\beta 3$  subunit  $\alpha 7$  helix in the

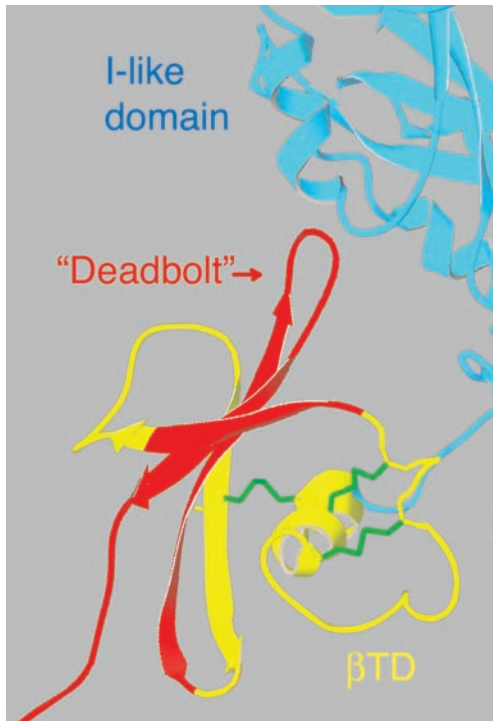


**Figure 8.** Ribbon diagram of the  $\beta$ -terminal domain of  $\beta 3$  (from Xiong *et al.*, 2001), showing structures expected to be missing in  $\beta 8$  (red). The deleted sequences include those that comprise the “deadbolt” that has been hypothesized to interact with the I-like domain and stabilized the bent, inactive conformation (Xiong *et al.*, 2003). Stabilizing disulfides that are retained in  $\beta 8$  are indicated in green.

“high-affinity” position did not by itself drive heterodimers into an extended conformation (Luo *et al.*, 2004). We agree with Takagi *et al.* (2002) that cellular regulation is probably mediated primarily by adjusting the bent-extended equilibrium. Extended heterodimers can then sample the open and closed conformations, and the stabilization of the open state by ligand binding can trigger integrin clustering, cellular signaling, and other downstream effectors. In any case, our data provide genetic support for the idea that hydrophobic interactions involving the  $\alpha 7$  and  $\alpha 1$ - $\alpha 1'$  helices of the  $\beta$  subunit I-like domain regulate integrin activity, in a manner analogous to that shown for  $\alpha$  subunit I domains (e.g., Xiong *et al.*, 2000).

Finally, the important complementary nature of forward genetics and site-directed mutagenesis is illustrated by a recent article reporting an alanine-scanning mutagenesis of the  $\beta 1$  I-like domain helices  $\alpha 1$ - $\alpha 1'$  and  $\alpha 7$  (Barton *et al.*, 2004). Although these authors did not check the residue corresponding to our  $mys^{b58}$  allele, they did alter the two hydrophobic residues in the  $\alpha 1$  helix region that make a partially exposed pocket for the  $mys^{b58}$  homologue of  $\beta 1$  in the closed conformation. These changes had little effect on activation in their assay system, but we would predict that changing these residues to polar amino acids (instead of alanines) would likely result in a more active integrin.

### **$\beta 8$ : The Exception that Proves the Rule?**

When comparing 25  $\beta$  subunit sequences from sponges to humans, only vertebrate  $\beta 8$  does not have a hydrophobic residue in the position homologous to that mutated in  $mys^{b58}$  (Moyle *et al.*, 1991); in  $\beta 8$  this residue is asparagine.  $\beta 8$

integrins have been reported to have broad ligand-binding capabilities and appear to function in the nervous system, in vascular morphogenesis, and regulation of cell growth (Nishimura *et al.*, 1994, 1998; Venstrom and Reichardt, 1995; Cambier *et al.*, 2000; Zhu *et al.*, 2002), but little is known about the regulation of  $\beta 8$  integrins in situ.

The presence of a highly polar residue in the  $mys^{b58}$  position led us to take a closer look at the rest of the  $\beta 8$  sequence. Xiong *et al.* (2003) have hypothesized that a loop in the membrane proximal “ $\beta$  terminal domain” of  $\beta$  subunits interacts with the I-like domain and serves as a “deadbolt” to stabilize the bent conformation of inactive heterodimers. Sequence comparisons reveal that the deadbolt structure is specifically deleted in  $\beta 8$  (Figure 8), and like the presence of a polar residue in the  $mys^{b58}$  position,  $\beta 8$  is unique among the 25 reported  $\beta$  subunits for this deletion. (Additionally,  $\beta 8$  is missing the otherwise completely conserved aspartates that coordinate the ADMIDAS cation [Xiong *et al.*, 2001, 2002], which apparently mediates tertiary structural changes of the I-like domain [Chen *et al.*, 2003; Mould *et al.*, 2003b]). The  $mys^{b58}$ -like polymorphism and lack of a deadbolt lead to the prediction that  $\beta 8$  containing integrins are activated very easily, perhaps constitutively. In any case, the comparisons indicate that the  $mys^{b58}$  mutation has identified an important side chain with physiological relevance in regulating integrin function.

### **ACKNOWLEDGMENTS**

We are extraordinarily indebted to many individuals who helped with the screens and other genetics and sequencing of mutants, including Irene Alvarez, Emily Brower, Melissa Davis, Marty Glansberg, Stefanie Hager, Wyatt Ho, Augustine Lau, Kirsten Metz, Ryan Reese, Michael Rhee, Jeff Rosenberger, Rick Salatino, Priyanka Sundareshan, Stephanie Tang, and especially Michael Zavortink. This work was supported by grants from the National Institutes of Health and the Arizona Disease Control Research Commission. We give thanks to the sequencing facility of the GATC at the University of Arizona, to Carl Boswell for help with the confocal microscopy, to Mark Ginsberg for help in design and construction of cytoplasmic mutants and for comments on the manuscript, to Anne Cress for help with the adhesion assays, to Marc Brabant for advice, and to Ted Wright for sharing unpublished data. Those who contributed fly stocks or other reagents include Eric Wieschaus, Ted Wright, Norbert Perrimon, Nick Brown, Mani Ramaswami and the Bloomington Stock Center. The authors have no competing financial interests.

### **REFERENCES**

- Ashburner, M. (1989). *Drosophila: A Laboratory Handbook*. Cold Spring Harbor, NY: Cold Spring Harbor Laboratory Press.
- Baker, S.E., Lorenzen, J.A., Miller, S.W., Bunch, T.A., Jannuzi, A.L., Ginsberg, M.H., Perkins, L.A., and Brower, D.L. (2002). Genetic interaction between integrins and *moleskin*, a gene encoding a *Drosophila* homologue of Importin-7 (DIM-7). *Genetics* 162, 285–296.
- Barton, S.J., Travis, M.A., Askari, J.A., Buckley, P.A., Craig, S.E., Humphries, M.J., and Mould, A.P. (2004). Novel activating and inactivating mutations in the integrin  $\beta 1$  subunit A domain. *Biochem. J.* 380, 401–407.
- Beglova, N., Blacklow, S.C., Takagi, J., and Springer, T.A. (2002). Cysteine-rich module structure reveals a fulcrum for integrin rearrangement upon activation. *Nat. Struct. Biol.* 9, 282–287.
- Bloor, J.W., and Brown, N.H. (1998). Genetic analysis of the *Drosophila*  $\alpha PS2$  integrin subunit reveals discrete adhesive, morphogenetic and sarcomeric functions. *Genetics* 148, 1127–1142.
- Brower, D.L., and Jaffe, S.M. (1989). Requirement for integrins during *Drosophila* wing development. *Nature* 342, 285–287.
- Brower, D.L., Wilcox, M., Piovant, M., Smith, R.J., and Reger, L.A. (1984). Related cell-surface antigens expressed with positional specificity in *Drosophila* imaginal discs. *Proc. Natl. Acad. Sci. USA* 81, 7485–7489.
- Brower, D.L. (2003). Platelets with wings: the maturation of *Drosophila* integrin biology. *Curr. Opin. Cell Biol.* 15, 607–613.

- Brown, N.H., King, D.L., Wilcox, M., and Kafatos, F.C. (1989). Developmentally regulated alternative splicing of *Drosophila* integrin PS2  $\alpha$  transcripts. *Cell* 59, 185–195.
- Bunch, T.A., and Brower, D.L. (1992). *Drosophila* PS2 integrin mediates RGD dependent cell-matrix interactions. *Development* 116, 239–247.
- Bunch, T.A., Graner, M.W., Fessler, L.I., Fessler, J.H., Schneider, K.D., Kerschen, A., Choy, L.P., Burgess, B.W., and Brower, D.L. (1998). The PS2 integrin ligand tigrin is required for proper muscle function in *Drosophila*. *Development* 125, 1679–1689.
- Bunch, T.A., Miller, S.W., and Brower, D.L. (2004). Analysis of the *Drosophila*  $\beta$ PS subunit indicates that regulation of integrin activity is a primal function of the C8–C9 loop. *Exp. Cell Res.* 294, 118–129.
- Bunch, T.A., Salatino, R., Engelsgerd, M.C., Mukai, L., West, R.F., and Brower, D.L. (1992). Characterization of mutant alleles of *mysospheroid*, the gene encoding the  $\beta$  subunit of the *Drosophila* PS integrins. *Genetics* 132, 519–528.
- Cambier, S., Mu, D.Z., O'Connell, D., Boylen, K., Travis, W., Liu, W.H., Broadus, V.C., and Nishimura, S.L. (2000). A role for the integrin  $\alpha$ v $\beta$ 8 in the negative regulation of epithelial cell growth. *Cancer Res.* 60, 7084–7093.
- Chen, J., Salas, A., and Springer, T.A. (2003). Bistable regulation of integrin adhesiveness by a bipolar metal ion cluster. *Nat. Struct. Biol.* 10, 995–1001.
- Costello, W.J., and Thomas, J.B. (1981). Development of thoracic muscles in muscle-specific mutant and normal *Drosophila melanogaster*. *Soc. Neurosci. Abstr.* 7, 543.
- Emsley, J., Knight, C.G., Farndale, R.W., Barnes, M.J., and Liddington, R.C. (2000). Structural basis of collagen recognition by integrin  $\alpha$ 2 $\beta$ 1. *Cell* 101, 47–56.
- Fogerty, F.J., Fessler, L.I., Bunch, T.A., Yaron, Y., Parker, C.G., Nelson, R.E., Brower, D.L., and Fessler, J.H. (1994). Tigrin, a novel *Drosophila* extracellular matrix protein that functions as a ligand for  $\alpha$ PS2 $\beta$ PS integrins. *Development* 120, 1747–1758.
- Gloor, G.B., Preston, C.R., Johnson-Schlitz, D.M., Nassif, N.A., Phillis, R.W., Benz, W.K., Robertson, H.M., and Engels, W.R. (1993). Type I repressors of P element mobility. *Genetics* 135, 81–95.
- Graner, M.W., Bunch, T.A., Baumgartner, S., Kerschen, A., and Brower, D.L. (1998). Splice variants of the *Drosophila* PS2 integrins differentially interact with RGD-containing fragments of the extracellular proteins tigrin, ten-m, and D-laminin 2. *J. Biol. Chem.* 273, 18235–18241.
- Hantgan, R.R., Paumi, C., Rocco, M., and Weisel, J.W. (1999). Effects of ligand-mimetic peptides arg-gly-asp-X (X = phe, trp, ser) on  $\alpha$ IIb $\beta$ 3 integrin conformation and oligomerization. *Biochemistry* 38, 14461–14474.
- Hantgan, R.R., Rocco, M., Nagaswami, N., and Weisel, J.W. (2001). Binding of a fibrinogen mimetic stabilizes integrin  $\alpha$ IIb $\beta$ 3's open conformation. *Protein Sci.* 10, 1614–1626.
- Hynes, R.O. (2002). Integrins: bidirectional allosteric signaling machines. *Cell* 110, 673–687.
- Jannuzzi, A.L., Bunch, T.A., Brabant, M.C., Miller, S.W., Mukai, L., Zavortink, M., and Brower, D.L. (2002). Disruption of C-Terminal cytoplasmic domain of  $\beta$ PS integrin subunit has dominant negative properties in developing *Drosophila*. *Mol. Biol. Cell* 4, 1352–1365.
- Kamata, T., Ambo, H., Puzon-McLaughlin, W., Tieu, K.K., Handa, M., Ikeda, Y., and Takada, Y. (2004). Critical cys residues for regulation on integrin  $\alpha$ IIb $\beta$ 3 are clustered in the EGF domains of the  $\beta$ 3 subunit. *Biochem. J.* 378, 1079–1082.
- Lee, J.O., Rieu, P., Arnaout, M.A., and Liddington, R. (1995). Crystal structure of the A domain from the subunit of integrin CR3 (CD11b/CD18). *Cell* 80, 631–638.
- Lewis, E.B., and Bacher, F. (1968). Methods of feeding ethyl methane sulfonate (EMS) to *Drosophila* males. *Dros. Inf. Serv.* 43, 193.
- Liddington, R.C., and Ginsberg, M.H. (2002). Integrin activation takes shape. *J. Cell Biol.* 158, 833–839.
- Lindsley, D.L., and Zimm, G.G. (1992). *The Genome of Drosophila melanogaster*. San Diego, CA: Academic Press.
- Liu, S., Calderwood, D.A., and Ginsberg, M.H. (2000). Integrin cytoplasmic domain binding proteins. *J. Cell Sci.* 113, 3563–3571.
- Lu, C., Shimaoka, M., Ferzly, M., Oxvig, C., Takagi, J., and Springer, T.A. (2001). An isolated, surface-expressed I domain of the integrin L2 is sufficient for strong adhesive function when locked in the open conformation with a disulfide. *Proc. Natl. Acad. Sci. USA* 98, 2387–2392.
- Luo, B.H., Springer, T.A., and Takagi, J. (2003a). Stabilizing the open conformation of the integrin headpiece with a glycan wedge increases affinity for ligand. *Proc. Natl. Acad. Sci. USA* 100, 2403–2408.
- Luo, B.-H., Springer, T.A., and Takagi, J. (2003b). High affinity ligand binding by integrin does not involve head separation. *J. Biol. Chem.* 278, 17185–17189.
- Luo, B.-H., Takagi, J., and Springer, T.A. (2004). Locking the  $\beta$ 3 integrin I-like domain into high and low affinity conformations with disulfides. *J. Biol. Chem.* 279, 10215–10221.
- Manseau, L. *et al.* (1997). GAL4 enhancer traps expressed in the embryo, larval brain, imaginal discs and ovary of *Drosophila*. *Dev. Dynam.* 209, 1–13.
- Martin-Bermudo, M.D., Dunin-Borkowski, O.M., and Brown, N.H. (1998). Modulation of integrin activity is vital for morphogenesis. *J. Cell Biol.* 141, 1073–1081.
- Martin, D., Zusman, S., Li, X., Williams, E.L., Khare, N., DaRocha, S., Chiquet-Ehrismann, R., and Baumgartner, S. (1999). Wing blister, a new *Drosophila* laminin  $\alpha$  chain required for cell adhesion and migration during embryonic and imaginal development. *J. Cell Biol.* 145, 191–201.
- Mould, A.P., Askari, J.A., Barton, S., Kline, A.D., McEwan, P.A., Craig, S.E., and Humphries, M.J. (2002). Integrin activation involves a conformational change in the  $\alpha$ 1 helix of the  $\beta$  subunit A-domain. *J. Biol. Chem.* 277, 19800–19805.
- Mould, A.P., Barton, S.J., Askari, J.A., McEwan, P.A., Buckley, P.A., Craig, S.E., and Humphries, M.J. (2003a). Conformational changes in the integrin  $\beta$ A domain provide a mechanism for signal transduction via hybrid domain movement. *J. Biol. Chem.* 278, 17028–17035.
- Mould, A.P., Barton, S.J., Askari, J.A., Craig, S.E., and Humphries, M.J. (2003b). Role of ADMIDAS cation-binding site in ligand recognition by integrin  $\alpha$ 5 $\beta$ 1. *J. Biol. Chem.* 278, 51622–51629.
- Moyle, M., Napier, M.A., and McLean, J.W. (1991). Cloning and expression of a divergent integrin subunit  $\beta$ 8. *J. Biol. Chem.* 266, 19650–19658.
- Nishimura, S.L., Boylen, K.P., Einheber, S., Milner, T.A., Ramos, D.M., and Pytela, R. (1998). Synaptic and glial localization of the integrin  $\alpha$ v $\beta$ 8 in mouse and rat brain. *Brain Res.* 791, 271–282.
- Nishimura, S.L., Sheppard, D., and Pytela, R. (1994). Integrin  $\alpha$ v $\beta$ 8; interaction with vitronectin and functional divergence of the  $\beta$ 8 cytoplasmic domain. *J. Biol. Chem.* 269, 28708–28715.
- O'Toole, T.E., Katagiri, Y., Faull, R.J., Peter, K., Tamura, R., Quaranta, V., Loftus, J.C., Shattil, S.J., and Ginsberg, M.H. (1994). Integrin cytoplasmic domains mediate inside-out signal transduction. *J. Cell Biol.* 124, 1047–1059.
- Shimaoka, M., and Springer, T.A. (2003). Therapeutic antagonists and conformational regulation of integrin function. *Nat. Rev. Drug Discov.* 2, 703–716.
- Sun, Q.H., Liu, C.Y., Wang, R., Paddock, C., and Newman, P.J. (2002). Disruption of the long-range GPIIIa Cys5–Cys435 disulfide bond results in the production of constitutively active GPIIb–IIIa ( $\alpha$ IIb $\beta$ 3) integrin complexes. *Blood* 100, 2094–2101.
- Takagi, J., Petre, B.M., Walz, T., and Springer, T.A. (2002). Global conformational rearrangements in integrin extracellular domains in outside-in and inside-out signaling. *Cell* 110, 599–611.
- Venstrom, K., and Reichardt, L. (1995).  $\beta$ 8 integrins mediate interactions of chick sensory neurons with laminin-1, collagen IV, and fibronectin. *Mol. Cell Biol.* 6, 419–431.
- Wieschaus, E.C., Nusslein-Volhard, C., and Jurgens, G. (1984). Mutations affecting the pattern of the larval cuticle in *Drosophila melanogaster* III. Zygotic loci on the X chromosome. *Roux's Arch. Dev. Biol.* 193, 296–307.
- Wilcox, M. (1990). Genetic analysis of the *Drosophila* PS integrins. *Cell Diff. Dev.* 32, 391–400.
- Wright, T.R.F. (1968). Phenogenetics of temperature sensitive alleles of *lethal mysospheroid* in *Drosophila*. *Proc. 12th Int. Congr. Genet.* 1, 41.
- Xiong, J.P., Li, R., Essafi, M., Stehle, T., and Arnaout, M.A. (2000). An isoleucine-based allosteric switch controls affinity and shape shifting in integrin CD11b A-domain. *J. Biol. Chem.* 275, 38762–38767.
- Xiong, J.-P., Stehle, T., Diefenbach, B., Zhang, R., Dunker, R., Scott, D.L., Joachimiak, A., Goodman, S.L., and Arnaout, M.A. (2001). Crystal structure of the extracellular segment of integrin  $\alpha$ v $\beta$ 3. *Science* 294, 339–345.
- Xiong, J.-P., Stehle, T., Goodman, S.L., and Arnaout, M.A. (2003). New insights into the structural basis of integrin activation. *Blood* 102, 1155–1159.
- Xiong, J.-P., Stehle, T., Zhang, R., Joachimiak, A., Frech, M., Goodman, S.L., and Arnaout, M.A. (2002). Crystal structure of the extracellular segment of integrin  $\alpha$ v $\beta$ 3 in complex with an arg-gly-asp ligand. *Science* 296, 151–155.
- Xu, T., and Rubin, G.M. (1993). Analysis of genetic mosaics in developing and adult *Drosophila* tissues. *Development* 117, 1223–1237.

- Yang, W., Shimaoka, M., Chen, J.-F., and Springer, T.A. (2004a). Activation of integrin  $\beta$  subunit I-like domains by one-turn C-terminal helix deletions. *Proc. Natl. Acad. Sci. USA* *101*, 2333–2338.
- Yang, W., Shimaoka, M., Salas, A., Takagi, J., and Springer, T.A. (2004b). Intersubunit signal transmission in integrins by a receptor-like interaction with a pull string. *Proc. Natl. Acad. Sci. USA* *101*, 2906–2911.
- Yee, G.H. (1993). Identification and characterization of integrin receptor subunits in *Drosophila melanogaster*. PhD Thesis, Cambridge: Massachusetts Institute of Technology.
- Zavortink, M., Bunch, T.A., and Brower, D.L. (1993). Functional properties of alternatively spliced forms of the *Drosophila* PS2 integrin  $\alpha$  subunit. *Cell Adhes. Commun.* *1*, 251–264.
- Zhu, J., Motejlek, K., Wang, D., Zang, K., Schmidt, A., and Reichardt, L.F. (2002).  $\beta 8$  integrins are required for vascular morphogenesis in mouse embryos. *Development* *129*, 2891–2903.
- Zusman, S., Grinblat, Y., Yee, G., Kafatos, F.C., and Hynes, R.O. (1993). Analyses of PS integrin functions during *Drosophila* development. *Development* *118*, 737–750.